Electronic Supplementary Material (ESI) for ChemComm.

Supporting information

Modulating the Optical Properties of Carbon Dots by Peptide Condensates

Dor Gaash,[a] Simran Dewan [a], Avigail Baruch Leshem[a], Kumar Sagar Jaiswal[b-c], Raz Jelinek[b-c], and Ayala Lampel*[a,d-f]

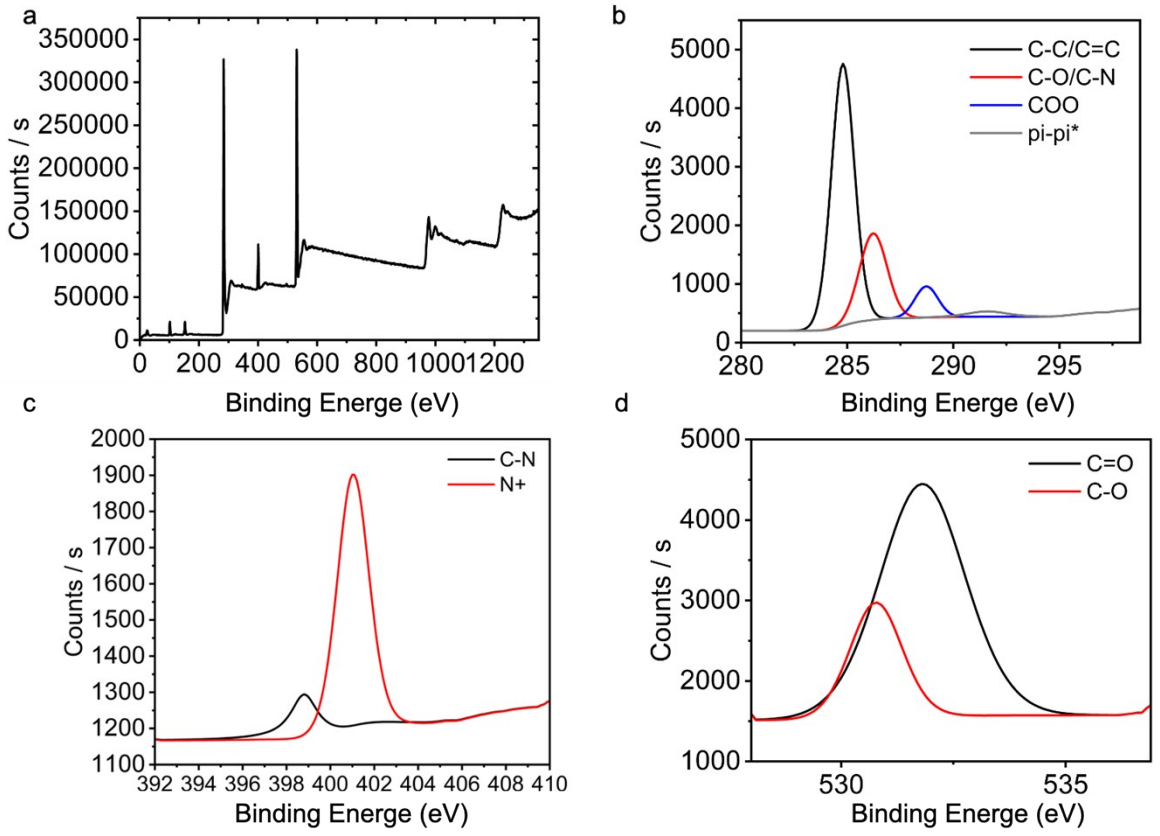

Figure S1. XPS analysis of the YCDots. a. Full scan survey of YCDots. **b-d**. Indicated peaks for C1s (**b**), N1s (**c**), and O1s (**d**).

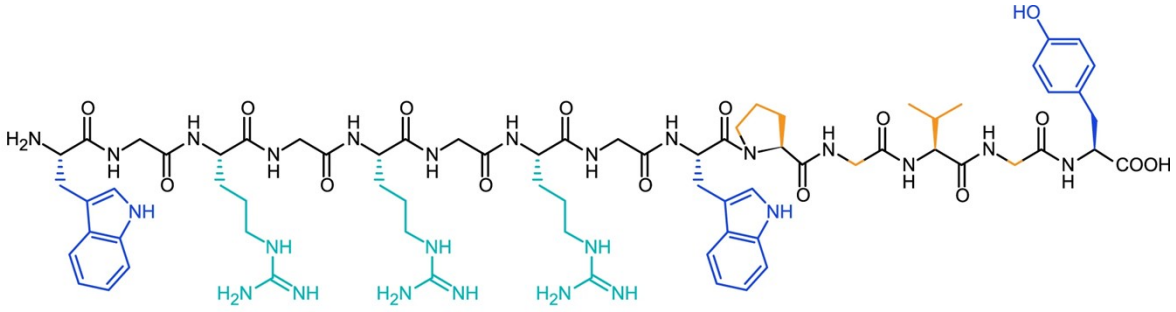

Figure S2. Chemical structure of WGR-1 peptide. Color code: aromatic amino acid side chains in blue, basic amino acid side chains in turquoise and ELP domain side chains in orange.

Table S1. Reported encapsulation efficiency (%EE) of C-dots in different vehicles.

Type of Carbon Dot	Vehicle Composition	Method of %EE analysis	Observed %EE
Thiophene phenylpropionic acid (PPA) NIR C-dots[1]	Nano-liposomes	Ultrafiltration	88.7 ± 4.3%
Green fluorescent C-dots[2]	Chitosan-based Hydrogel	Centrifugation	54.56 ± 2.03%
C-dots prepared by top down approach using carbon powder[3]	Protein conjugates	CD spectroscopy	88.46± 3.8%
Folic-acid derived C-dots[4]	Triazine dendrimer	Dialysis	84.28%

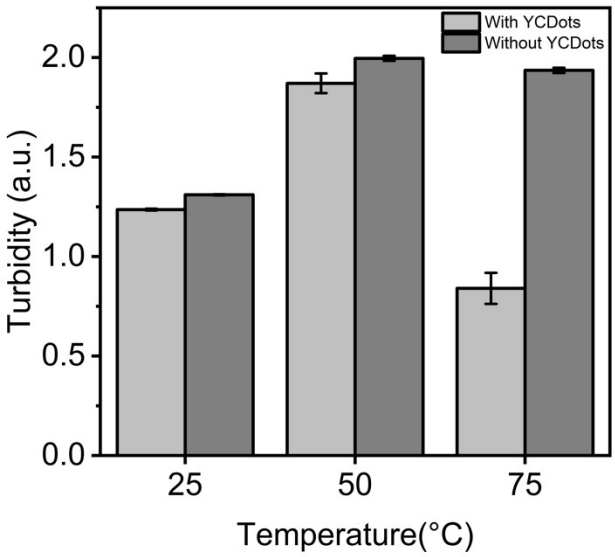

Figure S3. Turbidity analysis of peptide condensates with vs. without YCDots at varying temperature. The condensate samples were incubated for 10 min at the indicated temperatures. Values represent an average of n=3, error bars represent standard deviation.

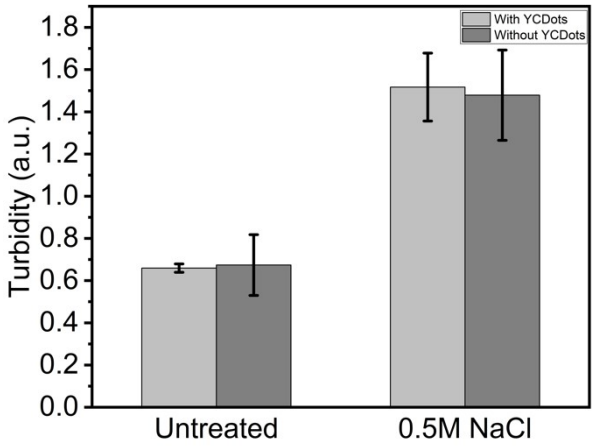

Figure S4. Turbidity analysis of peptide condensates with vs. without YCDots in the absence of presence of 0.5 M NaCl (final concentration). NaCl was added to pre-formed condensates. As a control, the same volume of DDW was added to the untreated condensates. Values represent an average of n=3, error bars represent standard deviation.

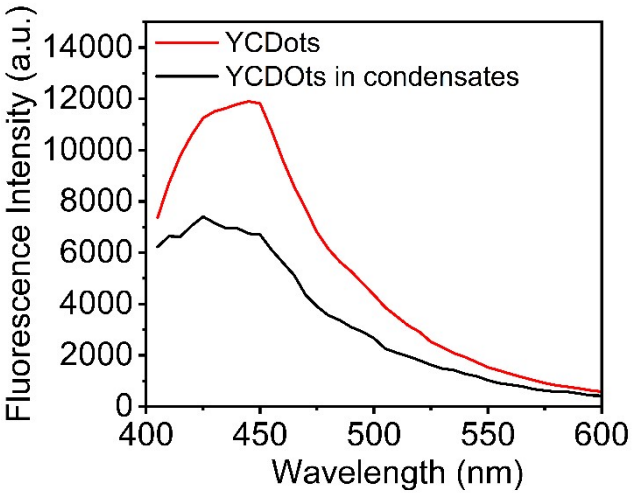

Figure S5. Fluorescence intensity of dissolved YCDots and YCDots partitioned in WGR-1 condensates.

Methods

YCDots synthesis

Carbon dots were synthesized as previously depicted (Bloch et al., 2020). 2 g of tyrosine and citric acid were mixed in a molar ratio of 6:1, and solubilized in 10mL DDW by titrating 32% HCl until the solution became clear. The solution was treated hydrothermally in a Teflon-lined autoclave at 215°C for 17 hours. The formed fluorescent dark solution was purified by centrifugation at 8000 RPM for 15 minutes, filtration of the supernatant via 220 nm Syringe filters, and 2-day dialysis in DDW. The solution was lyophilized until dried. The dark powder obtained was solubilized in DDW at a 0.5 mg/ml concentration for further characterization.

Preparation of peptide condensates

WGR-1 peptide was synthesized and purified by Genscript, Singapore. 20 mM solution of the peptide condensates was prepared in 20 mM phosphate buffer with 0.2 M NaCl at pH 7.5. The pH was adjusted to 7.5 so that the solution appeared turbid.

UV-Vis absorption spectroscopy analysis of YCDots

0.25 mg/ml solutions of YCDots, tyrosine, and citric acid were prepared in DDW as dispersive medium. UV-Vis absorbance spectra were measured in 1cm cells using a Cary 100 spectrophotometer, within the range 200-800 nm at 1 nm interval.

FT-IR analysis of YCDots

FT-IR spectra were recorded using attenuated total reflectance (ATR) with a diamond crystal, using Bruker Tensor 27 IR with a clean crystal recorded as blank for each sample. The absorbance spectra of carbon dots, tyrosine, and citric acid were measured within the range of 400-4000 cm^{-1}, using few milligrams of the original powder for each material.

Fluorescence spectroscopy analysis of YCDots

0.5 mg/ml YCDots fluorescence was measured in DDW as a dispersive medium at a volume of 45 µl, using a Horiba Jobin Yvon FL3-11 spectrofluorometer. Fluorescence emission spectra were recorded in the range of 375-600 nm at 5 nm intervals, upon excitation in the range of 350-450 nm.

Transmission electron microscopy (TEM)

A 5 µl aliquot of 0.5 mg/ml YCDots in DDW was placed on 400-mesh copper grids coated with a carbon-stabilized formvar film and incubated for 2 min. Excess solutions were removed by blotting the grid with a piece of filter paper and then the grid was left to air-dry. The sample

was viewed in a JEM-1400Plus TEM operating at 80 kV. Images were recorded using the SIS Megaview III camera, iTEM the Tem imaging platform (Olympus).

X-ray photoelectron spectroscopy (XPS) analysis of YCDots

Measurements were performed on YCDots powder using an ESCALAB QXi X-ray photoelectron spectrophotometer.

Encapsulation efficiency of YCDots in condensates

Tyrosine carbon dots were solubilized at a concentration of 0.5 mg/ml in 20 mM phosphate buffer with 200 mM NaCl, pH=7.5. Peptide-based condensates solution was prepared in the same buffer, once as previously described (Baruch Leshem et al., 2022), and once with the previously dissolved YCDots at 0.5 mg/ml. The solutions were pipetted, incubated for 10 minutes, and centrifuged at 1000 rpm for 10 minutes. Of the solutions mentioned, 3 replicates of 35 µl from the supernatant were aliquoted to a black 384-well plate. Fluorescence at 435 nm was recorded from each well upon excitation at 375nm by Biotek H1 synergy plate reader. Buffer was used as blank solution.

The concentration of the supernatant solutions was determined by a calibration curve, and the encapsulation efficiency (%EE) was calculated using the formula:

$$\%\mathrm{EE} = \frac{C_T - C_{\mathrm{sup}}}{C_T}$$

When C_T is the concentration of the YCDots stock solution And C_{sup} is the concentration of the supernatant upon centrifugation of YCDots partitioned in WGR-1 condensates.

The experiment was conducted and replicated (n=5).

Imaging of condensates

Peptide and peptide with YCDots condensates were imaged by Zeiss Zen LSM 900 inverted microscope with ×20/0.8 NA Plan- Apochromat air objective. Samples were prepared and imaged using a 96-well Black Glass bottom plate, glass 1.5H. Images were taken at crop of x10. Fluorescent images were taken using a λex=405 nm laser. The range of the histogram was equalized to 0-20000 for images to maintain consistency. The fluorescence intensity was calculated using Zen lite and the histograms for both samples were plotted using OriginLab. N=20 condensates of the same diameter (~2.8-2.9 µm) were taken for analysis after normalization from the dilute phase, for both peptide and peptide with YCDots condensate samples.

Images of condensates over time (Figure 4) were taken using via brightfield mode using fluorescence microscope (Inverted motorized microscope, Olympus), x60/0.95 NA Universal Plan Extended Apochromat objective. Images were collected and processed using Cellsens Dimension software (Olympus).

Time-dependent fluorescence

0.5 mg/ml YCDots were solubilized in 20 mM phosphate buffer with 0.2 M NaCl, pH=7.5. Peptide-based droplets at 20 mM were prepared in the phosphate buffer, either with or without the carbon dots. The solutions were incubated for 10 min. Of each solution, 35 µl triplicates were aliquoted to a black 384-well plate. Fluorescence spectra were recorded over time from each well via Biotek H1 synergy plate reader upon excitation at λ_{ex}=375 nm, within the range 390-700 nm at intervals of 5 nm. The fluorescence for phosphate buffer was subtracted from the fluorescence of the corresponding well for each solution. For solutions of peptide with YCDots, the fluorescence of the peptide solution was subtracted. The experiments were repeated in quadruplicates.

References

1. W. Ren, S. Chen, Y. Liao, S. Li, J. Ge, F. Tao, Q. Huo, Y. Zhang and Z. Zhao, *Colloids and Surfaces B: Biointerfaces*, 2019, **174**, 384–392.
2. A. Sachdev, I. Matai and P. Gopinath, *Colloids and Surfaces B: Biointerfaces*, 2016, **141**, 242–252.
3. Z. Peng, S. Li, X. Han, A. O. Al-Youbi, A. S. Bashammakh, M. S. El-Shahawi and R. M. Leblanc, *Analytica Chimica Acta*, 2016, **937**, 113–118.
4. S. Karimi and H. Namazi, *New J. Chem.*, 2021, **45**, 6397–6405.
5. D. N. Bloch, S. Ben Zichri, S. Kolusheva and R. Jelinek, *Nanoscale Adv.*, 2020, **2**, 5866–5873.
6. A. Baruch Leshem, S. Sloan-Dennison, T. Massarano, S. Ben-David, D. Graham, K. Faulds, H. E. Gottlieb, J. H. Chill and A. Lampel, *Nat Commun*, 2023, **14**, 421.